https://doi.org/10.22226/2410-3535-2022-4-343-349

The effect of alloying and fluorination on the oxidation behavior of β-solidifying γ-TiAl based alloys

L. R. Shaikhutdinova, V. M. Imayev†, D. M. Trofimov, R. M. Imayev

†vimayev@mail.ru

Institute for Metals Superplasticity Problems, RAS, Ufa, 450001, Russia

The present work is devoted to study of the oxidation behavior of two β-solidifying γ-TiAl alloys (Ti-43.5Al-4Nb-1Mo-0.1B (TNM alloy) and Ti-44Al-6(Nb, Zr, Hf)-0.15B (TNZ alloy) (at.%)). The as-cast alloys were subjected to upset forging and heat treatment that resulted in similar microstructures in both alloys. Plate-shaped samples were cut from the obtained workpieces, mechanically polished and subjected to oxidation exposure at 800°C (500 h). The samples during annealing were periodically removed from the furnace and weighed. After oxidation exposure the mass gain of the TNZ sample was found appreciably smaller than that of the TNM sample. The preliminary fluorination treatment in a diluted hydrofluoric acid (HF) provided a noticeable increase of the oxidation resistance in the case of the TNM alloy and a significant worsening of the oxidation resistance in the case of the TNZ alloy. At the same time, the non-fluorinated sample of the TNZ alloy showed near the same oxidation resistance as the TNM samples subjected to preliminary fluorination treatment. EDS analysis revealed the competitive formation of aluminum and titanium oxides on the surfaces of the oxidized TNM and TNZ samples. Predomination of the alumina formation contributed to higher oxidation resistance.

Keywords: gamma titanium aluminides, β-solidifying TiAl alloys, microstructure, oxidation resistance, fluorination treatment.

1. Introduction

Intermetallic alloys based on the γ(TiAl) + α_2(Ti_3Al) phases (hereafter called as TiAl alloys) are lightweight high-temperature materials, which have recently been applied as blade materials in modern aircraft engines instead of conventional nickel base superalloys [1, 2]. Their maximum operating temperature is generally limited to 700 – 750°C [3]. One of the critical issues of TiAl alloys is insufficient oxidation resistance, which impedes the use of these alloys at higher temperatures. Long-term exposure at 650 – 900°C causes undesirable embrittlement in different TiAl alloys, which is known as a surface related issue [4 – 6]. Oxidation of TiAl alloys at 700 – 900°C leads to formation of a mixed oxide scale consisting of TiO_2 and Al_2O_3 even in case of heavily alloyed TiAl alloys. Both oxides embrittle the alloy but TiO_2 in contrast to Al_2O_3 poorly impedes the penetration of oxygen into the bulk of material. At the same time, Al_2O_3 plays the role of the protective surface oxide scale. It is known that first of all the α_2(Ti_3Al) phase is prone to oxidation. The fact is that the solubility of oxygen in the α_2(Ti_3Al) phase is 10 – 20 at.%, whereas in the γ(TiAl) phase is only 1 – 3 at.% [5, 7]. The solubility of oxygen in the β(β_o) phase (which is present in TiAl alloys containing β stabilizers) is also higher than in the γ phase. In addition, the β(β_o) → α_2 phase transformation can lead to an increased oxygen content in the near-surface layer, which even after exposure at 600 – 700°C can cause the effect of embrittlement [6].

The generally accepted benchmark for evaluating the oxidation resistance of TiAl alloys is the mass gain for 1000 hours of exposure at a potential operating temperature at a level of <1 mg/cm^2 [8]. To improve the oxidation behavior of TiAl alloys at $T \leq 800$°C, alloying with such elements as niobium, tantalum, zirconium, molybdenum, tungsten and surface modification are usually considered, which should suppress the formation of titanium oxide (TiO_2). To protect against oxidation at $T \geq 850$°C, a protective coating is created on the surface of TiAl alloys [8].

In the present work, alloying and surface fluorination in a diluted hydrofluoric acid (HF) are considered to protect the surface from oxidation. As has been earlier established [8, 9], fluorination promotes the formation of a thin protective layer of Al_2O_3, which prevents the penetration of oxygen into the bulk of the material. Two β-solidifying TiAl alloys were taken as starting materials. The first alloy is the so called TNM alloy having a composition Ti-43.5Al-4Nb-1Mo-0.1B (at.%), and the second one is the recently designed TiAl alloy having a composition Ti-44Al-6(Nb, Zr, Hf)-0.15B (at.%). The first alloy along with the γ(TiAl) and α_2(Ti_3Al) phase contains also an appreciable amount of the β(β_o) phase due to alloying with Mo, which is known as a strong β stabilizer. The second alloy is near completely consists of the γ(TiAl) and α_2(Ti_3Al) phase due to excluding Mo and alloying with Zr and Hf, which are significantly weaker β stabilizers than Mo.

2. Materials and experimental

The following TiAl alloys were studied (at.%): Ti-43.5Al-4Nb-1Mo-0.1B and Ti-44Al-6(Nb, Zr, Hf)-0.15B (TNM and TNZ alloy, respectively). The alloys were produced

via arc-melting as ingots with an approximate weight of 100 g. The ingots were remelted at least ten times to attain good chemical homogeneity in the ingots. Energy dispersive X-ray (EDS) analysis showed that the ingot compositions were very close to the nominal compositions.

The as-cast ingots were subjected to upset forging at T=950°C to a strain of $\varepsilon \approx 30\%$ and low strain rates as described in our previous work [10]. As a result, sound forgings free of any cracks were obtained. The forged workpieces were subjected to the heat treatment, which included annealing at T=1250°C (2 h) (TNM) or 1270°C (2 h) (TNZ), followed by furnace cooling and annealing at T=900°C (4 h). Note that the heat treatment was fulfilled in the same furnace and the cooling rate after first annealing was near the same in both alloys. From the forged and heat treated workpieces 4 samples per alloy with a size of 20×12×1 mm were cut by spark cutting. All surfaces of the samples were mechanically polished down to a 4000 grit finish using SiC paper. The samples were cleaned with ethanol, rinsed with distilled water and dried in air prior to further studies. Two (non-treated) samples (a sample per alloy) were exposed isothermally in a furnace at 800°C for 500 h, and six samples (three samples per alloy) before exposure at 800°C were subjected to surface fluorination. To do it, the samples were immersed in an aqueous solution of 0.02–0.1 wt.% hydrofluoric acid (HF) for 0.5–1 h at room temperature. The fluorination time was longer in the case of a more diluted solution. During annealing at 800°C the samples were periodically inspected and weighed using an analytical balance with an accuracy of 10^{-6} g. As a result, the dependencies of the mass gain (in mg/cm^2) on time were drawn.

Microstructure examination was performed for the samples annealed for 500 h using a scanning electron microscope Tescan Mira-3 equipped with energy-dispersive X-ray spectroscopy (EDS). The sizes of the $\gamma+\alpha_2$ colonies and the γ grains, the volume fractions of the microstructure constituents were evaluated using images obtained in the back-scattering electron (BSE) mode. Post-oxidation microstructure and EDS analyses were carried out from the cross sections of samples. To do it, the oxidized samples were cased with Wood's metal casting and mechanically polished.

3. Results and discussion

3.1. Initial microstructures

Fig. 1 represents the BSE images of the alloys after upset forging and heat treatment. As mentioned, the TNM alloy contains three main phases, γ, α_2 and $\beta(\beta_o)$, and the resulting microstructure in the TNM alloy consists of $\gamma+\alpha_2$ lamellar colonies, γ grains having a dark contrast and $\beta(\beta_o)+\alpha_2$ grains/layers having bright and grey contrast, respectively. Taking into account that the fraction of the $\beta(\beta_o)+\alpha_2$ grains/layers is rather low, this microstructure can be interpreted as a near duplex structure consisting of $\gamma+\alpha_2$ lamellar colonies and γ grains. The TNZ alloy near completely consisted of two phases, γ and α_2, and the obtained microstructure is the duplex structure consisting of $\gamma+\alpha_2$ lamellar colonies and γ grains. In both alloys, there is also a small amount of borides crushed as a result of forging.

Microstructure features of the processed alloys are provided in Table 1. The fraction of lamellar colonies in the alloys was near the same. The lamellae width was not measured for the lamellar constituents but it was assumed that the same cooling rate applied after first annealing in both alloys resulted in near the same width of the lamellae. Thus, very similar microstructures were obtained in the treated alloys. This allows us to elucidate the effect of alloying on the oxidation resistance.

Table 1. Processing and microstructure features of workpieces of the Ti-43.5Al-4Nb-1Mo-0.1B and Ti-44Al-6(Nb,Zr,Hf)-0.15B alloys (d_m is the mean colony/grain size).

Alloy	Processing	Type of the microstructure	Microstructure constituents / the sizes of microstructure constituents, μm
TNM	Upset forging + heat treatment	Near duplex	70 vol.% $\gamma+\alpha_2$ colonies, d_m = 24 μm + about 25 vol.% γ grains, d_m = 8 μm + about 5 vol.% $\beta(\beta_o)+\alpha_2$ grains
TNZ	Upset forging + heat treatment	Duplex	65 vol.% $\gamma+\alpha_2$ colonies, d_m = 22 μm + about 35 vol.% γ grains, d_m = 9.5 μm + <0.5 vol.% $\beta(\beta_o)$ phase

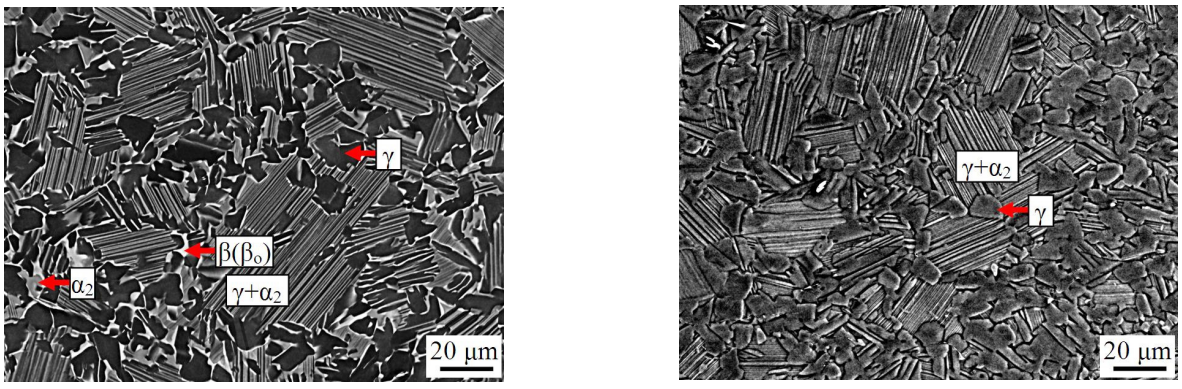

a b

Fig. 1. BSE images of the TNM and TNZ alloys obtained after upset forging and heat treatment. The arrows show the microstructure constituents.

3.2. Mass gain experiments

Fig. 2 displays the mass changes depending on oxidation time obtained for the non-treated and HF-treated TNM and TNZ samples, which were exposed to air at 800°C. The fluorination treatment was performed in 0.02%HF solution (60 min), 0.04%HF solution (45 min) and 0.1%HF solution (30 min). The mass gains for the non-treated samples of the TNM and TNZ alloys are 1.214 and 0.704 mg/cm^2, respectively. Alloying with Nb + Zr + Hf instead of Nb + Mo leads to a decrease in the mass gain after 500 h exposure at 800°C in 1.72 times. The approximation of the curves obtained for the non-treated samples up to 1000 h gives the mass gain values ≈2.1 and ≈1.1 mg/cm^2 for the TNM and TNZ alloy, respectively. Thus, the non-treated sample of the TNM alloy has insufficient oxidation resistance at 800°C from the viewpoint of the benchmark value assumed for evaluating the oxidation resistance of TiAl alloys whereas the non-treated sample of the TNZ alloy showed almost acceptable oxidation resistance (only slightly higher than the benchmark value of 1 mg/cm^2 after 1000 h exposure).

The fluorine treatment significantly improves the oxidation resistance of the TNM samples (Fig. 2 a). The mass gain for the TNM sample subjected to fluorination in the 0.4%HF solution is 2 times smaller than for the non-treated sample (0.6 mg/cm^2 vs. 1.21 mg/cm^2 after 500 h oxidation). On the contrary, the fluorination treatment of TNZ samples leads to an appreciable worsening of oxidation resistance (Fig. 2 b). The mass gain obtained after 500 h oxidation of the fluorinated TNZ samples is 0.968 – 1.238 mg/cm^2 against 0.704 mg/cm^2 in the case of the non-treated TNZ sample.

Thus, the fluorination treatment has significant positive impact on the oxidation resistance at 800°C in the TNM alloy but has also a negative impact on that in the TNZ alloy. Note that the fluorinated samples of the TNM alloy have approximately the same oxidation resistance as the non-treated sample of the TNZ alloy (0.6 – 0.705 mg/cm^2 vs. 0.704 mg/cm^2 after oxidation for 500 h). The approximation of the mass gain curves obtained for the fluorinated TNM samples shows that all samples irrespective of the HF concentration have acceptable oxidation resistance (the mass gain smaller than 1 mg/cm^2) after oxidation at 800°C for 1000 h (Fig. 2 a). The approximation of the mass gain curves obtained for TNZ samples shows that only the non-treated sample has near acceptable oxidation resistance (≈1.1 mg/cm^2), whereas the fluorinated samples have the mass gain up to 2 mg/cm^2 (Fig. 2 b).

3.3. SEM analysis of sample surfaces after oxidation at 800°C.

Figs. 3 and 4 show the elemental maps obtained for the TNM and TNZ non-treated and fluorinated samples. The fluorination treatment in the 0.04%HF solution leads to a smoother and thinner oxidation layer in comparison with the non-treated sample in the case of the TNM alloy. The layer enriched with oxygen is approximately 2 times thicker in the non-treated TNM sample than in the TNM sample fluorinated in 0.04%HF solution (Fig. 3 a, d). In both samples of the TNM alloy oxidation was accompanied by depletion in aluminum in the subsurface layer but this layer was thicker in the non-treated sample (Fig. 3 b, e). The subsurface layer was also depleted in titanium in the non-treated sample, whereas this was not observed in the fluorinated sample (Fig. 3 c, f). On the contrary, the fluorination treatment gave the opposite result in the TNZ alloy. The layer enriched with oxygen was approximately 2 times thicker in the TNZ sample fluorinated by 0.1%HF solution than in the non-treated TNZ sample (Fig. 4 a, d). In both samples of the TNZ alloy the oxidation was accompanied by depletion in aluminum in the subsurface layer but this layer was thicker in the case of the fluorinated sample (Fig. 4 b, e). The subsurface layer was also depleted in titanium in the fluorinated sample, whereas this was not observed in the non-treated sample (Fig. 4c, f).

Figs. 5 and 6 illustrate concentration profiles obtained for oxidized surfaces of the TNM and TNZ samples after oxidation at 800°C. The concentration maximum followed by concentration minimum of aluminum is observed on the oxidation surfaces of all samples. This suggests that alumina is formed on the oxidation surfaces of the samples. Titanium near the oxidation surface monotonically (or near monotonically) increases with some shift in relation to aluminum in the preliminary fluorinated TNM sample and the non-treated TNZ sample (Figs. 5 b and 6 a), whereas sawtooth dependence of the titanium concentration is observed near the oxidation surface in the non-treated

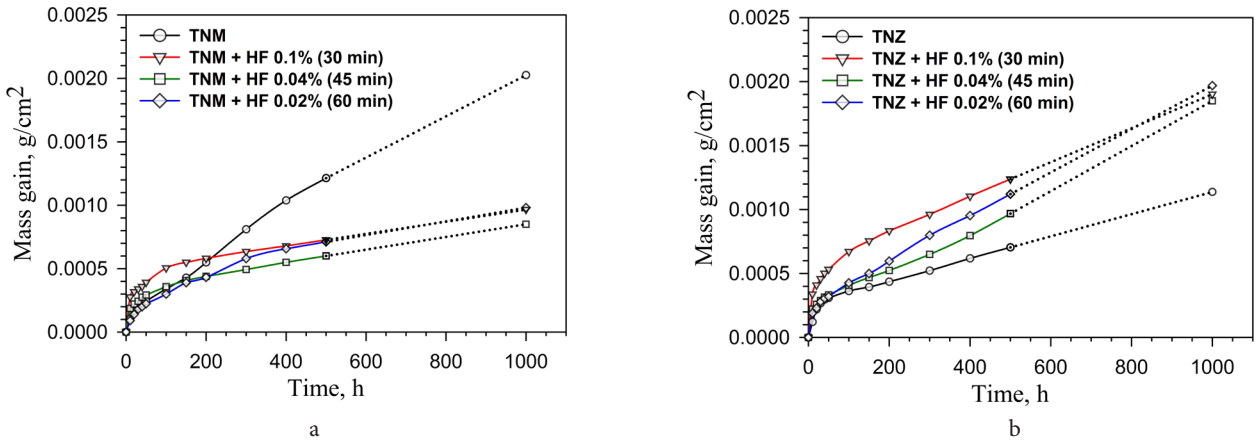

Fig. 2. (Color online) Mass gain depending on oxidation time of the TNM (a) and TNZ (b) samples, which were exposed to air at 800°C. The dotted lines show the approximation from 500 to 1000 h.

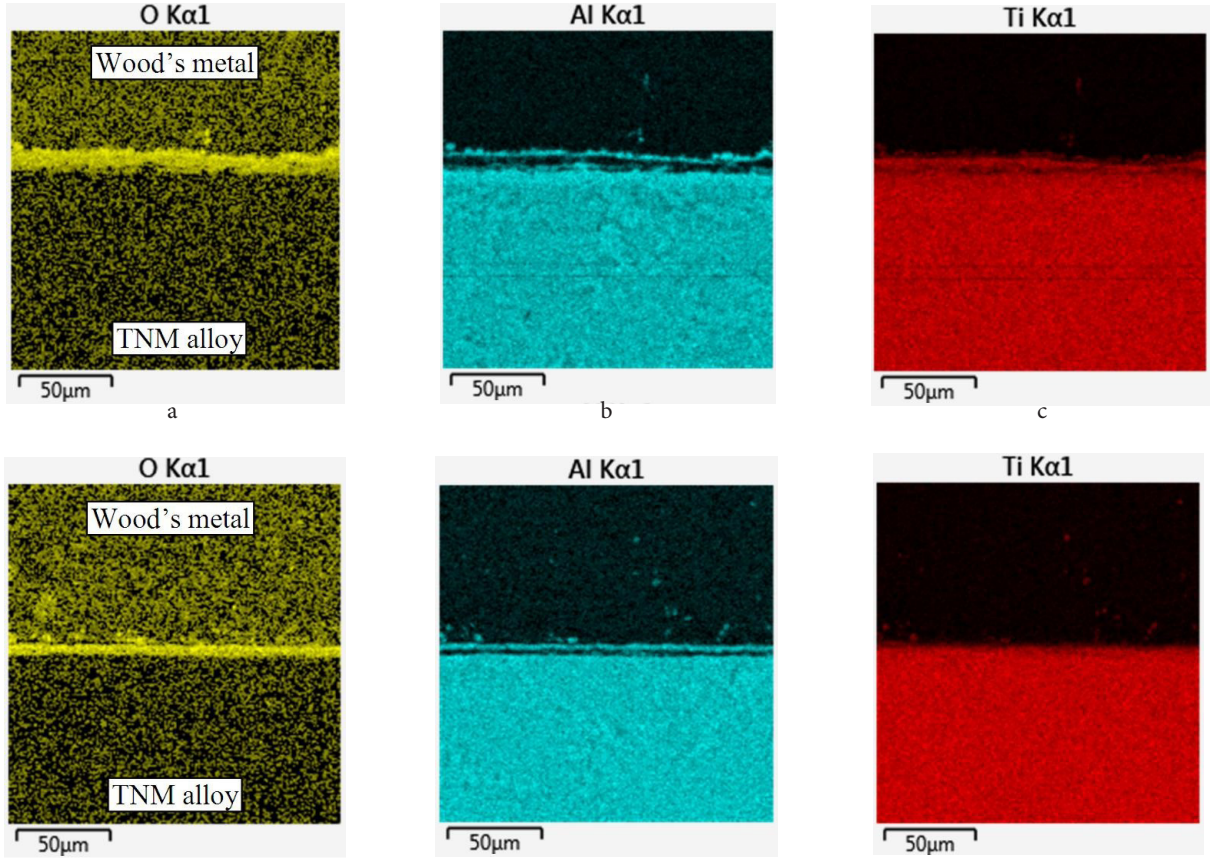

Fig. 3. (Color online) Elemental maps of the TNM samples after oxidation at 800°C (500 h): the non-treated sample (a – c), the sample after fluorination in 0.04%HF solution (d – f).

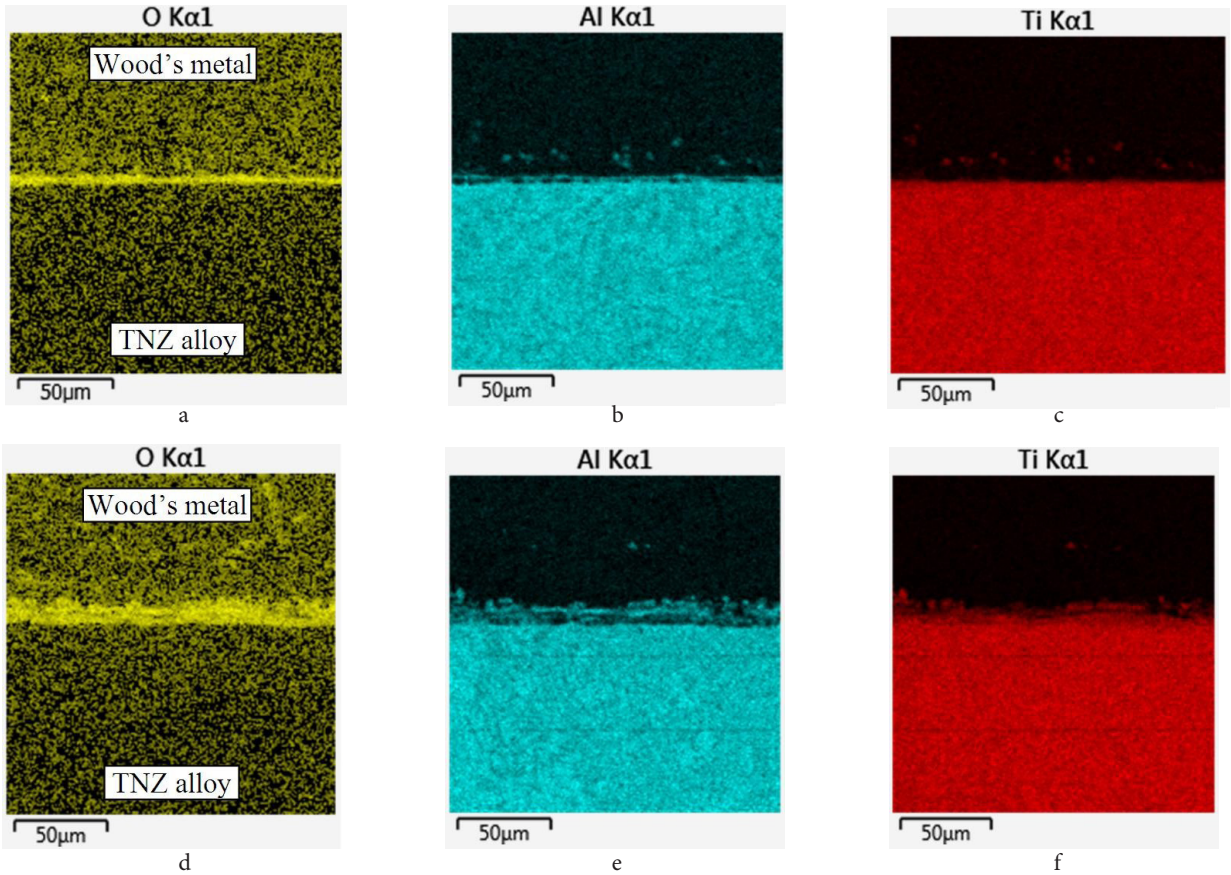

Fig. 4. (Color online) Elemental maps of the TNZ samples after oxidation at 800°C (500 h): the non-treated sample (a – c), the sample after fluorination in 0.1%HF solution (d – f).

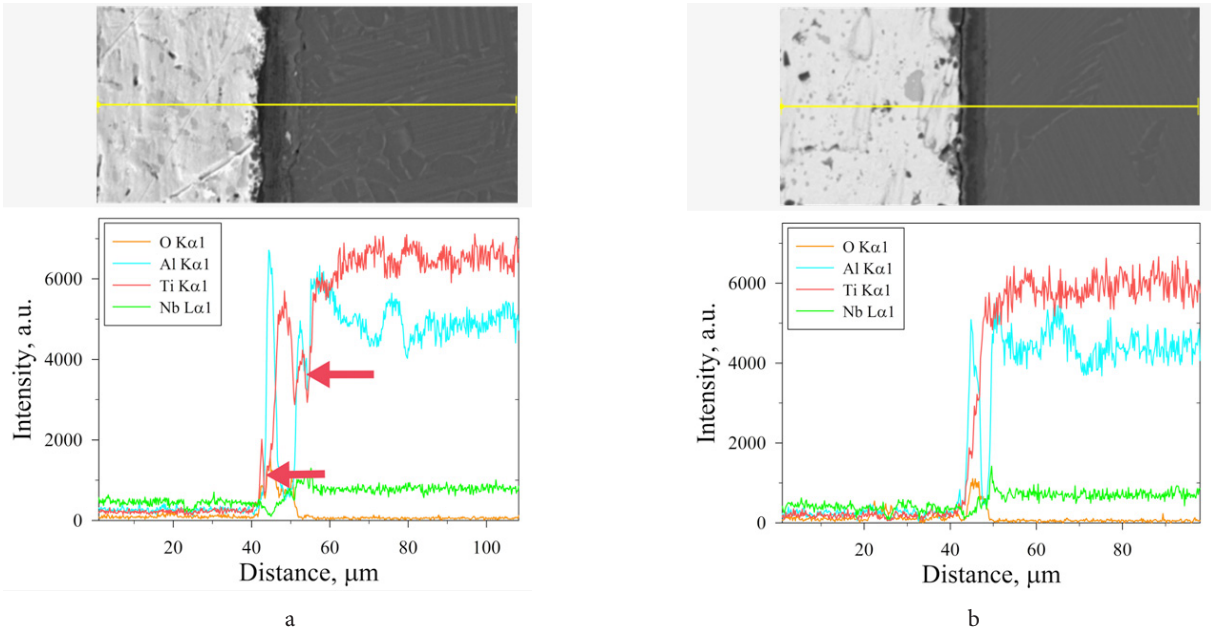

Fig. 5. (Color online) Concentration profiles obtained for oxidized surfaces of the TNM samples after oxidation at 800°C (500 h): the non-treated sample (a), the sample subjected to preliminary fluorination treatment in the 0.04% HF solution (b). The arrows show the sawtooth changes of the titanium concentration near the oxidation surface.

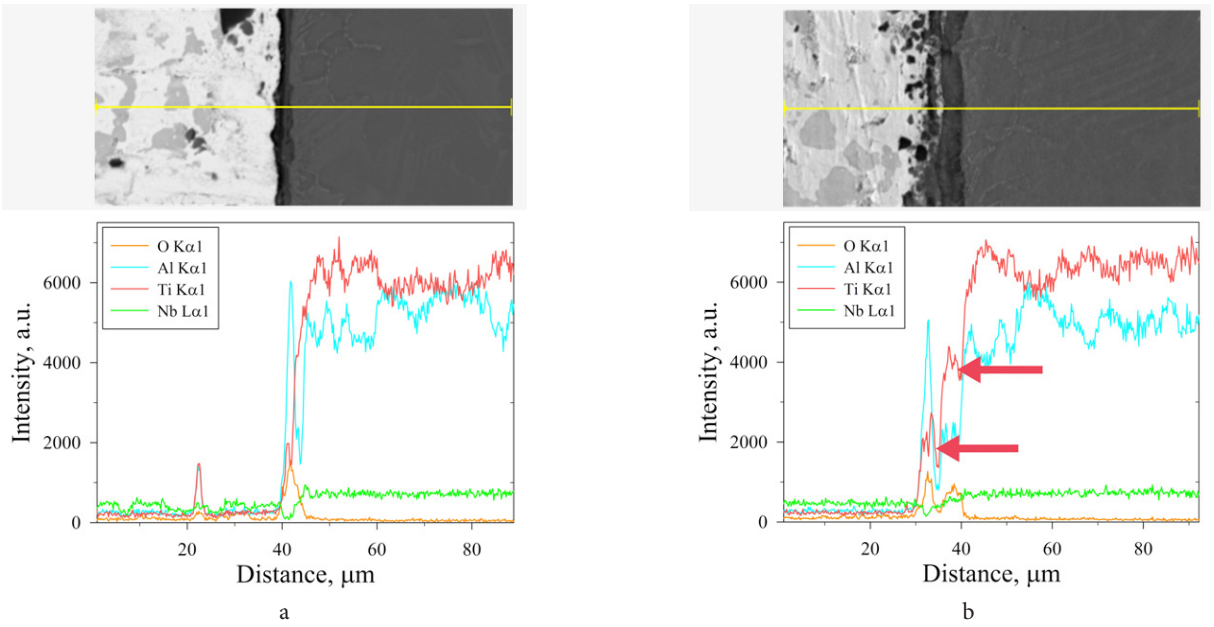

Fig. 6. (Color online) Concentration profiles obtained for oxidized surfaces of the TNZ samples after oxidation at 800°C (500 h): the non-treated sample (a), the sample subjected to preliminary fluorination treatment in the 0.1% HF solution (b). The arrows show the sawtooth changes of the titanium concentration near the oxidation surface.

TNM sample and the fluorinated TNZ sample (Figs. 5 a and 6 b). The latter suggests that diffusion of titanium occurs towards oxidation surface and it takes place together with aluminum diffusion (although to a lesser extend). Thus, the concentration profiles obtained near the oxidation surfaces show competitive oxidation of aluminum and titanium. First of all alumina is formed on the oxidation surface regardless of whether fluorination is carried out or not. However, the titanium oxide is also formed leading to depletion of the subsurface layer in titanium in the non-treated TNM and the fluorinated TNZ samples.

Fig. 7 represents the BSE images of the TNM and TNZ samples near the oxidation surfaces. The bright phase is observed near the oxidation surfaces. Taking into account that the oxidation subsurface is depleted in aluminum (as follows from the concentration profiles) one may suppose that the $\beta(\beta_o)$ phase is formed in the subsurfaces as a result of the phase transformations $\alpha_2 \rightarrow \beta(\beta_o)$ and $\gamma \rightarrow \beta(\beta_o)$. The continuous layer of the $\beta(\beta_o)$ phase is formed in the fluorinated TNM sample that is an indicative of the uniform depletion of the subsurface layer in aluminum. In the TNZ samples the $\beta(\beta_o)$ phase is formed despite the fact that alloying with Nb + Zr + Hf provides a lower β stabilization in the TNZ alloy than Nb + Mo in the TNM alloy. Slightly a higher amount of the $\beta(\beta_o)$ phase is formed in the non-treated TNZ sample in contrast to the fluorinated TNZ sample.

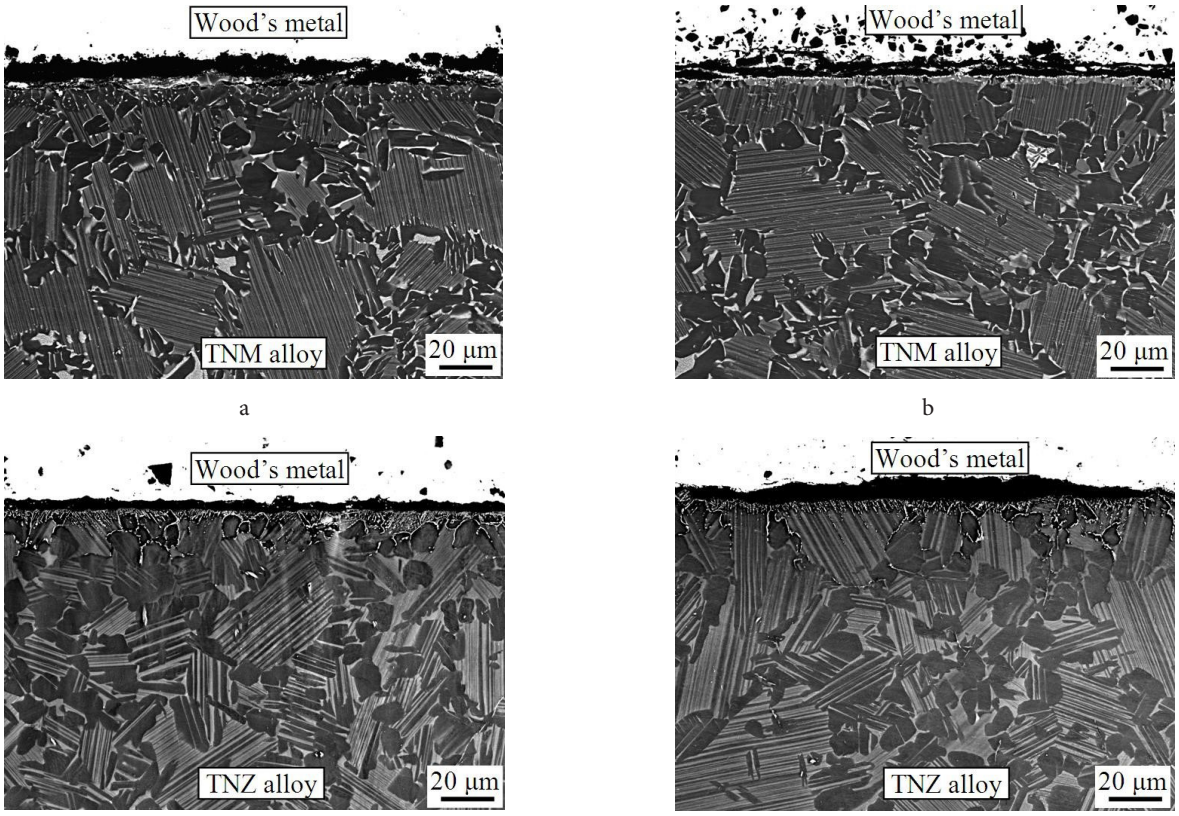

Fig. 7. BSE images of the TNM and TNZ samples near the oxidation surfaces after oxidation at 800°C (500 h): TNM alloy (a, b), TNZ alloy (c, d): the non-treated samples (a, c), the samples subjected to preliminary fluorination treatment in 0.04% HF and 0.1HF solutions, respectively (b, d).

Generally speaking, the formation of the β(β_o) phase in the subsurface layer is not favorable for oxidation resistance because of higher solubility of oxygen in the β(β_o) phase. At the same time, the formation of the β(β_o) phase indicates the depletion of the subsurface layer in aluminum, which is spent on the formation of alumina on the oxidation surface. Thus, the appearance of the β(β_o) phase can serve as an indicator of the alumina layer formation protecting against the penetration of oxygen into the material volume.

Thus, the fluorination treatment has a significant positive impact on the oxidation resistance at 800°C for the TNM alloy and comparable but a negative impact on the oxidation resistance for the TNZ alloy. It should be noted that the positive influence of the fluorination treatment on oxidation resistance was earlier revealed in different TiAl alloys, such as Ti-43.5Al-4Nb-1Mo-0.1B, Ti-48Al-2Nb-2Cr, Ti-48Al-2W-0.08B [11], Ti-43.5Al-4Nb-1Mo-0.1B, Ti-44Al-3Mo-0.1B, Ti-44Al-7Mo-0.09B [12]. The reason why fluorination has a negative effect on the oxidation resistance of the TNZ alloy at 800°C is currently unclear.

The results obtained allow us to conclude that alloying itself is essential for the oxidation resistance of TiAl alloys. After 500 h exposure at 800°C the mass gain of the non-treated TNZ sample was 1.72 times smaller than that of the non-treated TNM sample (0.704 against 1.214 mg/cm^2), although the quantity of the alloying elements (5 and 6 at.% in the TNM and TNZ alloy, respectively) and the initial microstructures were very similar. Most likely, some difference in the phase composition (first of all the presence of the β(β_o) phase in the TNM alloy) led to the instability of the phase composition upon holding at 800°C and contributed to the increased mass gain in the TNM sample.

EDS analysis revealed that long-term oxidation at 800°C led to the competitive formation of aluminum and titanium oxides on the surface of oxidized samples. If the formation of oxides was accompanied by depletion of the near-surface layer not only in aluminum, but also in titanium, then in this case the mass gain as a result of oxidation was higher than that in the case of depletion only in aluminum. The depletion in aluminum and titanium of the subsurface layer was observed in the non-treated TNM sample and the fluorinated TNZ samples, whereas the depletion in only aluminum was observed in the non-treated TNZ sample and the fluorinated TNM samples.

Note that various coatings including thermal barrier coatings were currently tried for TiAl alloys to protect against oxidation, such as $NbSi_2$, Al_2O_3, Y_2O_3, SiO_2, Ti-Al-Cr-Y-N, Ti-Al-Cr [8,13–17]. However, all investigated coatings are either not effective against oxidation or very likely lead to a strong degradation of mechanical properties (mechanical properties after coating are generally not studied). It is worth noting that the non-treated TNZ sample showed near the same oxidation resistance as the TNM sample after preliminary fluorination treatment in the (0.02 – 0.1)% HF solution. This indicates that reasonably chosen alloying of TiAl alloys may be sufficient to protect the alloy surface against oxidation at least up to 800°C. Further research is required to clarify this issue.

4. Conclusions

The following conclusions can be drawn:

- Similar near duplex and duplex type structures were obtained after upset forging and heat treatment in the Ti-43.5Al-4Nb-1Mo-0.1B (TNM) and Ti-44Al-6(Nb,Zr,Hf)-0.15B (TNZ) alloy, respectively. The plate-like samples of both alloys were subjected to oxidation at 800°C for 500 h. The mass gain experiments carried out during oxidation at 800°C (500 h) showed that the mass gain of the non-treated TNZ sample was 1.72 times lower than that of the non-treated TNM sample (0.704 and 1.214 mg/cm^2, respectively). Most likely, the presence of a small amount of the β(β_o) phase led to the instability of the phase composition upon holding at 800°C and contributed to the increased mass gain in the TNM sample. Approximation of the mass gain up to 1000 h give the values about 2.1 and 1.1 mg/cm^2 for the non-treated TNM and TNZ samples, respectively. This indicates that the TNZ alloy almost meets the requirements for oxidation at 800°C in contrast to the TNM alloy.

- The preliminary fluorination treatment in a diluted hydrofluoric acid (HF) provided a noticeable increase of the oxidation resistance in the TNM alloy and an appreciable decrease of the oxidation resistance in the TNZ alloy. The mass gain of the fluorinated TNM samples after oxidation at 800°C for 500 h decreased from 1.21 to 0.6 – 0.705 mg/cm^2, whereas the mass gain of the fluorinated TNZ samples increased from 0.704 to 0.968 – 1.238 mg/cm^2.

- Long-term oxidation at 800°C led to the competitive formation of aluminum and titanium oxides on the surfaces of the oxidized TNM and TNZ samples. EDS analysis revealed that if the formation of oxides was accompanied by depletion of the near-surface layer not only in aluminum, but also in titanium, then in this case the mass gain as a result of oxidation was higher than that in the case of depletion only in aluminum.

- The non-treated sample of the TNZ alloy showed near the same oxidation resistance as the TNM samples after preliminary fluorination treatment in the (0.02 – 0.1)% HF solution. This indicates that alloying of TiAl alloys may be sufficient to protect the alloy surface against oxidation at least up to 800°C.

Acknowledgements. The work was supported by the Ministry of Science and Higher Education of the Russian Federation according to the State Assignment of the IMSP RAS (No. AAAA-A17-117041310215-4). The work was performed using the facilities of the shared services center "Structural and Physical-Mechanical Studies of Materials" at the Institute for Metals Superplasticity Problems of Russian Academy of Sciences. The authors would like to thank Dr. N. Y. Parkhimovich for technical assistance.

References

1. B. P. Bewlay, S. Nag, A. Suzuki, M. J. Weimer. Mater. at High Temps. 33, 549 (2016). Crossref
2. P. Janschek. Materials Today: Proceedings. 2S, S92 (2015). Crossref
3. Y.-W. Kim, S. Kim. JOM. 70, 553 (2018). Crossref
4. X. Wu, A. Huang, D. Hu, M. H. Loretto. Intermetallics. 17, 540 (2009). Crossref
5. M. C. Galetz, A. S. Ulrich, C. Oskay, D. Faehsing, N. Laska, U. Schulz, M. Schuetze. Intermetallics. 123, 106830 (2020). Crossref
6. L. Mengis, A. S. Ulrich, P. Watermeyer, C. H. Liebscher, M. C. Galetz. Corrosion Science. 178, 109085 (2021). Crossref
7. P. Sallot, J. P. Monchoux, S. Jouli, A. Couret, M. Thomas. Intermetallics. 119, 106729 (2020). Crossref
8. R. Pflumm, S. Friedle, M. Schütze. Intermetallics. 56, 1 (2015). Crossref
9. S. Friedle, N. Nießen, R. Braun, M. Schuetze. Surface & Coatings Technology. 212, 72 (2012). Crossref
10. V. M. Imayev, A. A. Ganeev, D. M. Trofimov, N. Ju. Parkhimovich, R. M. Imayev. Mater. Sci. Eng. A. 817, 141388 (2021). Crossref
11. A. Donchev, L. Mengis, A. Couret, S. Mayer, H. Clemens, M. Galetz. Intermetallics. 139, 107270 (2021). Crossref
12. R. Pflumm, A. Donchev, S. Mayer, H. Clemens, M. Schütze. Intermetallics. 53, 45 (2014). Crossref
13. A. Sommer, Y. Zhang. Oral presentation P2-3 at the International conference GAT-2017, San-Diego, USA, Sept. 2011.
14. L.-K. Wu, W.-Y. Wu, J.-L. Song, G.-Y. Hou, H.-Z. Cao, Y.-P. Tang, G.-Q. Zheng. Corrosion Science. 140, 388 (2018). Crossref
15. M. Fröhlich, R. Braun, C. Leyens. Surface and Coatings Technology. 201, 3911 (2006). Crossref
16. N. Chaia, P. L. Cury, G. Rodrigues, G. C. Coelho, C. A. Nunes. Surface and Coatings Technology. 389, 125675 (2020). Crossref
17. L.-K. Wu, J.-J. Wu, W.-Y. Wu, G.-Y. Hou, H.-Z. Cao, Y.-P. Tang, H.-B. Zhang, G.-Q. Zheng. Corrosion science. 146, 18 (2019). Crossref